Marine Chemistry 262 (2024) 104395

Contents lists available at ScienceDirect

Marine Chemistry

journal homepage: www.elsevier.com/locate/marchem

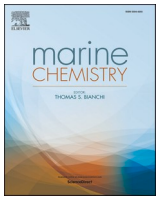

Microbial interactions with microplastics: Insights into the plastic carbon cycle in the ocean

Kai Ziervogel [a,*], Sierra Kehoe [a], Astrid Zapata De Jesus [a], Alireza Saidi-Mehrabad [b], Miriam Robertson [b], Ariana Patterson [c], Aron Stubbins [c,d]

[a] Institute for the Study of Earth, Oceans, and Space, University of New Hampshire, 8 College Road, Durham, NH 03824, USA
[b] Desert Research Institute, 755 East Flamingo Road, Las Vegas, NV 89119, USA
[c] Department of Marine and Environmental Sciences, Northeastern University, 39-41 Leon St, Boston, MA 02115, USA
[d] Departments of Civil and Environmental Engineering, and Chemistry and Chemical Biology, Northeastern University, 360 Huntington Avenue, Boston, MA 02115, USA

ARTICLE INFO

Keywords:
Microplastics
Plastic-derived DOC
Hydrolytic enzymes
Marine snow
Marine plastic snow

ABSTRACT

The fate of microplastics (MPs) in the ocean is mostly driven by (i) photo-oxidation to smaller particles and dissolved constituents, which fuel the dissolved organic carbon pool (plastic-derived DOC, pDOC), and (ii) interactions with organic matter forming sinking aggregates (marine plastic snow). Two separate laboratory experiments were conducted to investigate the two pathways of MPs. In the first experiment, we measured potential rates of microbial pDOC utilization in bottle incubations over 15 days with microbial assemblages from coastal and offshore waters. Microbial utilization of pDOC was more efficient in the coastal (72% bioreactive pDOC) compared with the offshore experiment (32% bioreactive pDOC) 15 days. Changes in bacterial cell abundance and extracellular enzyme activities (glucosidase, peptidase, esterases) indicated that a fraction of pDOC was repackaged into microbial exopolymeric substances (EPS), stimulating growth of known EPS degrading bacteria within the phyla Verrucomicrobiota and Planctomycetota. Microbial EPS likely also played a key role in our second experiment that showed the formation of marine plastic snow in roller tanks with cultured cells of *Emiliana huxleyi* but not with cells of an *Isocrysis* sp. culture. Average sinking velocities of marine plastic snow were a factor of 1.2 lower compared with marine snow without MPs. Both aggregate types showed reduced sinking velocities in a density stratified sinking column. Our results from the two experiments on (i) microbial utilization of pDOC and (ii) the formation and sinking of marine plastic snow indicate potential effects of plastic-derived compounds on microbial elemental cycles (i.e., pDOC repackaged into EPS) with consequences for the efficiency of the biological carbon pump (i.e., marine plastic snow reduces carbon export) and the fate of plastic-derived compounds in the ocean.

1. Introduction

Plastic contaminants in the ocean are dominated by particles of <5 mm in diameter known as microplastics (MPs), which are among the most widespread marine pollutants by means of relative abundances (Andrady, 2011; Stubbins et al., 2021). The mismatch between estimated inputs with observations of floating plastics indicate that plastics undergo biotic and abiotic degradation in the sea (Cózar et al., 2014; Law, 2017). Biodegradation of plastic debris in the ocean is slow (timescale of years) while photo-oxidation of plastics starts after days to weeks of UV radiation, and is thus considered the most effective transformation pathway of plastics in the environment (Gewert et al., 2015; Stubbins et al., 2021). Photo-oxidation of plastic debris results in the release of dissolved organic carbon (plastic-derived DOC, pDOC) composed of a broad range of molecular structures (Stubbins et al., 2023) potentially fueling microbial food webs. The few studies on microbial interactions with pDOC demonstrate the potential of heterotrophic microbes to use pDOC as energy sources (Romera-Castillo et al., 2018; Sheridan et al., 2022; Zhu et al., 2020); however, the extent of microbial degradation of pDOC may depend on background environmental factors (e.g., quality of natural DOM; Sheridan et al., 2022), plastic sources (Zhu et al., 2020), as well as levels of plastic additives that have been detected in marine environments at considerable concentrations with potential toxic effects for marine microbes

* Corresponding author.
E-mail address: kai.ziervogel@unh.edu (K. Ziervogel).

https://doi.org/10.1016/j.marchem.2024.104395
Received 6 October 2023; Received in revised form 18 April 2024; Accepted 21 April 2024
Available online 23 April 2024

(Hermabessiere et al., 2017; Zhu et al., 2020).

Another major loss pathway of floating MPs involves interactions with phytoplankton aggregates (marine snow), which change the buoyancy and thus sinking behavior of MPs (Galgani et al., 2022). Similar to MPs, marine snow are ubiquitous in the ocean (Alldredge and Silver, 1988; Simon et al., 2002), and sinking of marine snow-containing MPs (hereafter referred to as marine plastic snow) is a key parameter in global plastic inventories (Kvale et al., 2020). However, most of our knowledge on marine plastic snow comes from laboratory experiments with microbeads of <1 mm in size (Long et al., 2015; Michels et al., 2018a; Porter et al., 2018), which represent only a minor fraction of MPs accumulating in the surface ocean (Aoki and Furue, 2021).

This work contributes towards a better understanding of the two major pathways of MPs in surface waters: (i) microbial cycling of pDOC, and (ii) formation and sinking of marine plastic snow. For (i), we conducted bottle incubations with natural microbial assemblages from two contrasting marine environments (coastal vs. offshore) using pDOC amendments from photo-oxidized polypropylene, i.e., one of the most common plastics in the ocean (Andrady, 2011). In addition to changes in bacterial abundances and community structure in response to pDOC, we measured potential activities of extracellular enzymes using fluorogenic substrate proxies. Enzyme assays provide insights into the relative composition of substrates present in the investigated sample (Chrost, 1991). We targeted two esterases (oleate- and butyrate-hydrolyzing enzymes) as potential indicators for enzymatic breakdown of plastic polymers (Zhang et al., 2022) and other carboxylic acid-containing compounds, which are major components of pDOC (Gewert et al., 2015, 2018; Stubbins et al., 2023). We also measured potential activities of glucosidases and peptidases as indicators for microbial cycling of carbohydrates and peptides as major compounds of marine biopolymers (Repeta, 2015). For (ii), we conducted roller tank experiments with MPs (HDPE) and two phytoplankton cultures (*Emiliana huxleyi*, *Isochrysis* sp.) coupled with particle sinking velocity measurements in an unstratified and density stratified water column, to assess potential aggregation and sinking patterns of marine plastic snow under different hydrodynamic conditions. Collectively, the results from the two experiments reveal new insights into microbial interactions with plastic debris in the ocean.

2. Material and methods

2.1. Microbial degradation of pDOC

2.1.1. Photo-oxidation of plastics

Leachates of photo-oxidized polypropylene (PP) were used as plastic-derived DOC (pDOC) amendments in bottle incubations with seawater containing natural microbial assemblages. Prior to the bottle experiments, postconsumer PP was cleaned by sonication in Milli-Q, and photo-oxidized in a solar simulator equipped with 12 UVA-340 bulbs (Q-Panel) for 2 months at 25 °C to 30 °C, as described in Zhu et al. (2020). The wavelengths used in the simulator approximate natural solar irradiance (295 to 365 nm) responsible for most environmental photochemical reactions, including plastic photodegradation (Andrady et al., 1996; Stubbins and Dittmar, 2012; Zhenfeng et al., 1996). The incubation flasks (2-L ashed spherical quartz irradiation flasks filled with 1 L of Milli-Q) were repositioned daily to average potential spatial variation in the light flux under the solar simulator. Following photo-oxidation, the water was filtered through 0.22-μm filters (GVWP04700, Millipore-Sigma) to remove PP pieces, and the filtrate was stored frozen (−20 °C) until the beginning of the bioassays.

2.1.2. Bioassays of pDOC degradation

Water samples for pDOC bioassays were collected on the pier of the UNH Jackson Estuarine Laboratory (43°05′45”N 70°52′08”W) located on the shore of the Great Bay Estuary (hereafter referred to as the coastal site), and at a site about 40 miles off the coast of New Hampshire in the Gulf of Maine (42°51′41.04”N 69°51′41.04”W; hereafter referred to as offshore site) on October 18, 2021, and November 3, 2021, respectively. Coastal water was collected below the surface with a pre-rinsed bucket. Offshore water was taken at 1 m water depth with Niskin bottles on a CTD rosette deployed from RV Gulf Challenger. Prior to the start of the incubation, water samples were gravity filtered through a 1.2-μm filter to remove larger particles and grazers, retaining most microbes in the filtrate.

The two separate time course experiments with coastal and offshore waters were initiated within 24 h of sampling. Six 1-L pre-combusted Pyrex bottles were filled to the 1-L mark (total volume: 1.25 L) with seawater from the respective site containing natural microbial assemblages. Two additional bottles were prepared with 1.2-μm filtered and autoclaved seawater serving as abiotic controls. Three of the six live bottles and one of the control bottles were amended with pDOC (7 mL each bottle), yielding a final DOC concentration of about five times the background levels, which were assumed to be 200 μM and100 μM for the coastal and offshore site, respectively, at the time of sampling. The remaining bottles (three live and one control) received 7 mL of milli-Q instead of the pDOC amendment, thus serving as a non-pDOC control. The bottles were incubated in a climate-controlled room at in situ temperatures at the time of sampling (coastal: 16 °C; offshore: 13 °C) and in the dark to prevent primary production.

Six time points were taken on days 1, 3, 6, 8, 10, and 15 of the incubation. At each time point, 25 mL were removed from each experimental bottle and divided into separate vials and processed for DOC, bacterial cell counts, and hydrolytic enzyme activities as described below. After the final time point (day 15), the remaining volume of the replicate bottles (874 mL per bottle) were pooled and filtered onto 0.2-μm polycarbonate filter until the filters were clogged (total volume filtered per sample ~300 mL). Another set of 0.2-μm polycarbonate filters were prepared with the initial water from the two sites after sampling. The 0.2-μm polycarbonate filters from the initial and the final sampling were stored in liquid nitrogen for later analysis of microbial community composition (16S rRNA) as outlined below.

2.1.3. DOC analysis

Twenty mL samples were filtered through 0.2-μm surfactant free cellulose acetate (SFCA) syringe filters, acidified to pH <2 using HCl, and stored at 5 °C prior to analysis using a Shimadzu TOC-VCPH total organic carbon analyzer (Stubbins and Dittmar, 2012). DOC concentrations of the non-pDOC bottles were subtracted from those that received pDOC, to estimate pDOC concentrations at each of the time points. Microbial degradation of pDOC was described by a single, three parameter exponential decay model:

$$DOC(t) = DOC_{\infty} + z0^{-kt} \quad (1)$$

with DOC(t) = concentration of pDOC (μM) bottles at time point (t), DOC_{∞} = an adjustable parameter that represents the non-bioreactive DOC component (i.e., the DOC concentration that is predicted to survive at time equals infinity), z0 = an adjustable component that represents the concentration of bioreactive DOC at time = 0, k = the rate of decay, and t = the time (days). The relative proportion of bioreactive pDOC was derived from subtracting DOC_{∞} from DOC (day 1). Kinetics parameters were computed in JMP® 16.

2.1.4. Bacterial cell counts and extracellular enzyme activities

One mL samples for bacterial cell counts were fixed with a solution of 1% paraformaldehyde and 0.01% glutaraldehyde and stored in liquid nitrogen before enumeration using a flow cytometer (Miltenyi Biotec MACSQuant VYB) with SYBR green as a DNA stain (Gasol and Del Giorgio, 2000). Hydrolytic enzyme activities were determined using four structurally distinct fluorogenic substrate proxies (Hoppe, 1983). Three mL samples were pipetted into 4-mL acrylic cuvettes containing substrate stock solutions of 4-Methylumbelliferyl (MUF) β-D-glucopyranoside, L-Leucine-7-amido-4-methylcoumarin (MCA) hydrochloride,

4-MUF oleate and 4-MUF butyrate as substrates for glucosidase, peptidase, and two esterase enzymes, respectively. The final concentration for all four substrates was 200 μM (i.e., enzyme saturation level). The cuvettes were incubated in the dark at 16 °C and 13 °C for the coastal and offshore water experiment, respectively, and for up to 24 h. Fluorescence readings were taken at the beginning of the incubation and at two to three additional time points over the course of the incubation under buffered conditions (20 nM borate buffer; pH 10.2) using a Turner Biosystems TBS-380 fluorometer (excitation/emission channels set to "UV"; 365 nm excitation, 440–470 nm emission). Changes in fluorescence over time were used to calculated potential enzyme activities. Fluorescence readings were calibrated using MUF and MCA standard solutions.

2.1.5. Bacterial community analysis

Genomic DNA was extracted from 0.2-μm polycarbonate filters using the ZymoBIOMICS DNA Microprep kit (Zymo Research, USA), following Saidi-Mehrabad et al. (2020). Genomic DNA yield was checked with a Qubit 4.0 fluorometer and a high sensitivity dsDNA quantitation kit (Thermofisher USA). For amplicon sequencing, 16S rRNA genes from the V4 region of the samples was amplified using Earth Microbiome Primers 515F and 806R (Caporaso et al., 2012) and sequenced on a Novaseq PE250 platform (Illumina USA). Amplicon Sequence Variants (ASVs) were generated with DADA2 Pipeline (1.26) (Callahan et al., 2016) in R environment. In summary, the sequence truncation length was set to 125 bp for forward sequences and 150 bp for reverse sequences, which was determined based on the quality score distribution at each base position. At the filtering step, no "Ns" were allowed, and the maximum allowable number of expected errors was set to 2 and 5, respectively. On average, 98% of the filtered and trimmed sequences met our initial quality control criteria. The error rate for both forward and reverse sequences was determined from 514,099 reads obtained from 6 samples in total. A total of 4650 ASVs were inferred from merged sequences, of which 793 were flagged as chimeric. Removal of flagged ASVs resulted in 3857 filtered ASVs (98% retained). The taxonomic classification was performed via naïve Bayesian algorithm (Wang et al., 2007) with a Silva-trained database (138.1) formatted for the DADA2 (Pruesse et al., 2007). The minimum bootstrap was set to 70%. In addition to the Silva database, the taxonomic identity of the ASVs were verified using the National Center for Biotechnology Information database's standard nucleotide collection. Results matching our blank control or human microbiome, were removed from the dataset. Removal of the anomalous sequences resulted in a final set of 3805 ASVs (98.6% retained). The final ASV table was normalized to the lowest read count of 61,680 bp with the aid of MOTHUR pipeline (1.48.0) (Schloss et al., 2009). The sequences are registered in the NCBI SRA database (Bioproject ID: PRJNA1073994; coastal site: SAMN39848632, offshore site: SAMN39848633). The relative abundance analysis was conducted manually in Microsoft Excel® and differences among treatments were tested with the Mann–Whitney *U* test.

2.2. Aggregation and sinking of MPs

2.2.1. Roller tank incubations

Interactions between MPs and phytoplankton were investigated in roller tanks incubated on a roller table (Shanks and Edmondson, 1989). Cultures of *Emiliana huxleyi* (*E. hux*; CCMP371) and *Isochrysis* sp. (CCMP2164) were grown in F/2 medium at 22 °C in artificial seawater (31 PSU; Instant Ocean Sea Salt). The dense media (visual observation) were filled into replicate acrylic roller tanks (tank volume: 1 L; two tanks each culture). One of the tanks per culture received 25 pieces of MPs (high-density polyethylene – HDPE) while the other tank (no MPs) served as the non-plastic control. HDPE pieces were prepared from postconsumer plastic grocery bags with clean scissors (average area of plastic pieces: 2.4 mm^2 ± 0.8 mm^2). The tanks were incubated on a roller table at 2.5 rpm until marine snow-sized aggregates formed (~24 h after the start of the incubation). The tanks were then carefully removed from the roller table and placed upright to allow aggregates to settle to the bottom (30–40 min). Aggregates >1 mm (visually discernible) were randomly chosen and manually collected using a 10-mL pipette pump (SEOH) with a cut-off tip. Aggregates separated by treatment were placed into petri dishes pre-filled with 0.2-μm filtered tank water. The petri dishes were placed on top of a square grid and individual aggregates were photographed with a digital microscope (Carson eFlex) at 75× effective magnification. Images of the two-dimensional projection of the aggregates were processed using ImageJ software to determine the longest diameter for each aggregate.

2.2.2. Aggregate sinking measurements

Sinking velocities of aggregates were measured using two different approaches to simulate particle sinking in an unstratified and stratified water column. The first approach used a 10-mL pipette pump (SEOH) with a cut-off tip in which the aggregates were drawn into following their sizing. The aggregates were allowed to freely sink while recording the distance (2.54 cm) and time of the sinking process as described in Laurenceau-Cornec et al. (2015), who found only minor differences in sinking rates between the pipette method and a large sinking cylinder. For the second approach, a density stratified cylinder (10 cm wide x 10 cm deep x 50 cm tall dimensions) was prepared by filling the bottom part (20 cm) with 37 PSU artificial seawater. The top part of the tank contained artificial seawater with 31 PSU (Prairie et al., 2017). Aggregates were gently transferred by pipette below the surface of the top layer (one aggregate at a time) and recorded during sinking using a shadowgraph setup with a camera (Grasshopper 3, Teledyne FLIR), light source and specialized drafting paper for tracking particle settling (Mandel et al., 2020). Sinking velocities in the stratified water column were calculated from the entire sinking process through the surface layer and the density transition zone into the bottom layer of the column. The extent of stratification in the sinking cylinder was estimated using the Brunt-Väisälä frequency:

$$N = \sqrt{-\frac{g}{\rho 0}\frac{\delta\rho}{\delta z}} \quad (2)$$

with $\rho 0$ = 1025.50 kg m^{-3} (fluid density of lower layer), and $\delta\rho$ = 1020.95 kg m^{-3} – 1025.50 kg m^{-3} (fluid density of upper layer - fluid density of lower layer). The thickness of the transition layer (δz) was estimated to be 1 cm based on the sinking behavior of the aggregates at the transition layer.

3. Results

3.1. Biodegradation of pDOC

The decrease of pDOC of time followed 1st order decay kinetics in both experiments (coastal and offshore) albeit at different rates. In the coastal water experiment, 72% of the pDOC was degraded ($p < 0.0001$; 95% $CI_{asymptote}$ [139.3, 244.4]) while only 32% pDOC was utilized in the offshore experiment ($p < 0.005$; 95% $CI_{asymptote}$ [275.4, 314.4]; Fig. 1). The time course of pDOC degradation differed between the two experiments, showing a gradual decrease throughout the incubation time in the coastal water bottles (Fig. 1a). In contrast, pDOC in the offshore bottles decreased in the first week and remained constant until day 15 (Fig. 1b). DOC in the unamended treatments showed only minor variations over time in both experiments (Table 1).

3.2. Changes in bacterial cell numbers and enzyme activities in response to pDOC

Bacterial cell numbers in the coastal water pDOC treatment increased by a factor of 1.5 in the first week followed by minor changes in the second week (Table 1). Bacterial cell numbers in the offshore

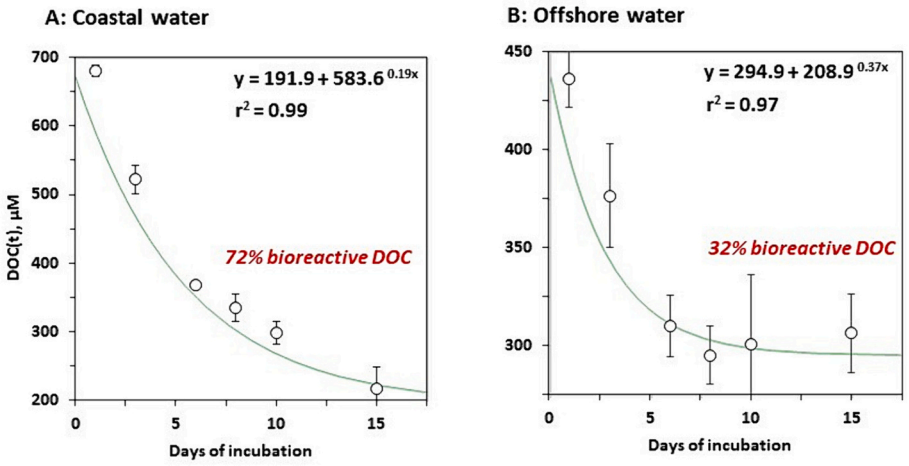

Fig. 1. Changes in average pDOC concentrations ($n = 3 \pm$ standard deviations) over time in the experimental bottles with (A) coastal water and (B) offshore water. Changes in pDOC followed 1st order decay kinetics (fitting line).

Table 1
Bacterial cell abundance (mL^{-1}), dissolved organic carbon (DOC, µM), and enzyme activities (nM h^{-1}) in the experimental bottles with coastal and offshore waters, containing natural levels of DOC (unamended) and plastic-derived DOC (pDOC, amended). Values are averages of replicate bottles (n = 3 ± standard deviations, in parentheses). PEP – peptidase, GLU – glucosidase, n.d. - not detectable.

			Days of incubation					
			1	3	6	8	10	15
Bacterial cells*10^5	Coastal	Unamended	3.8 (0.9)	4.1 (0.6)	3.5 (0.2)	5.2 (2.7)	5.0 (2.0)	3.6 (1.1)
		Amended	7.9 (3.4)	10.8 (1.8)	11.6 (5.5)	8.8 (2.0)	12.3 (9.4)	11.3 (5.1)
	Offshore	Unamended	7.6 (9.3)	1.8 (0.8)	1.9 (0.9)	2.7 (1.8)	1.2 (0.5)	1.2 (0.3)
		Amended	1.5 (0.9)	3.0 (2.4)	2.2 (0.9)	5.0 (4.9)	9.9 (11.0)	24.6 (36.4)
DOC	Coastal	Unamended	197 (27.6)	203 (21.6)	190 (26.6)	178 (18.6)	177 (15.5)	190 (3.8)
		Amended	869 (8.4)	711 (20.6)	557 (2.7)	524 (20.5)	488 (16.9)	406 (31.2)
	Offshore	Unamended	114 (15.3)	95 (25)	117 (6.2)	114 (2.3)	106 (34.1)	88 (24.1)
		Amended	542 (14.3)	482 (26.4)	416 (15.5)	401 (14.7)	406 (35.3)	412 (20)
PEP	Coastal	Unamended	1195 (245.1)	1476 (283.2)	474.3 (227.4)	352.1 (134.6)	322.3 (99.6)	316.6 (143.1)
		Amended	465.9 (307.7)	2102 (367)	2354 (113)	1125 (671.3)	330.7 (137.5)	227.2 (103.6)
	Offshore	Unamended	61.4 (17.9)	1249 (392.2)	1404 (457.7)	1519 (314.4)	1300 (906)	412 (127.6)
		Amended	n.d.	832.5 (43.9)	738.5 (33.8)	956.2 (170.1)	1552 (801.2)	1054 (426.7)
GLU	Coastal	Unamended	5.5 (0.6)	5.7 (3.1)	2.4 (0.8)	1.9 (0.7)	2.7 (0.1)	3.5 (0.9)
		Amended	5.0 (0.8)	6.3 (0.5)	7.0 (7.3)	10.0 (3.4)	7.1 (4.9)	8.4 (4.9)
	Offshore	Unamended	3.5 (0.3)	53.3 (2.8)	55 (3.3)	61.8 (3.6)	40 (24.1)	1.9 (0.9)
		Amended	n.d.	57.4 (16.4)	57.6 (23.7)	87 (21.4)	52.8 (12.2)	23.7 (8.9)
Esterase (oleate)	Coastal	Unamended	520.6 (220.8)	252.4 (79.6)	176.2 (43.8)	136.1 (13.3)	114.7 (28.8)	30.45 (1.85)
		Amended	304.7 (26.8)	139.9 (12.6)	173.1 (126)	135.4 (99)	45.1 (16.4)	7.0 (15.3)
	Offshore	Unamended	5.7 (1.3)	105.8 (17)	70.2 (7.7)	55.1 (7.7)	45.1 (4.3)	24.9 (3.2)
		amended	2.5 (1.1)	56 (15.7)	24.7 (13.5)	34.2 (7.1)	31.4 (11.1)	34.4 (18.8)
Esterase (butyrate)	Coastal	Unamended	1088 (418.7)	1487 (275)	815.7 (136.4)	1185 (83.2)	683.8 (90.5)	328.2 (11.9)
		Amended	472.8 (32.5)	891.5 (82.1)	1022 (205.1)	993.6 (255.5)	693.6 (47.9)	287.1 (82.1)
	Offshore	Unamended	279.6 (0.8)	1156 (148.7)	814.1 (53.2)	849.7 (19)	658.2 (214)	199.2 (5.3)
		Amended	169.8 (4.4)	827 (115.5)	741.6 (192)	997.2 (149.2)	1066 (210.4)	551.2 (178.9)

pDOC treatment showed a five-fold increase in the second week of the incubation. Cell numbers in both unamended treatments remained low throughout the time course of the incubations.

Enzyme activities expressed as the ratio between the pDOC and the unamended treatments, showed distinct substrate- and site-specific patterns (Fig. 2). Peptidase and glucosidase activities in the coastal pDOC treatment surpassed those of the unamended treatment by day 3, reaching up to 7 times higher rates compared with the unamended

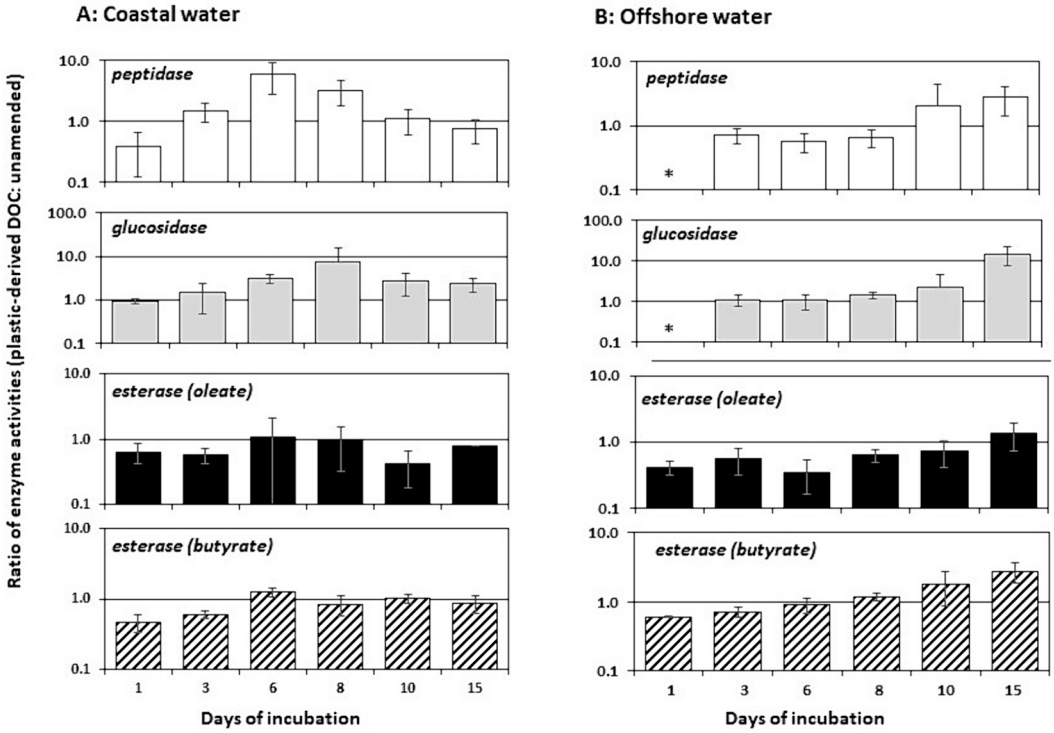

Fig. 2. Differences in potential enzyme activities (n = 3 ± standard deviations) over time in the experimental bottles with (A) coastal water and (B) offshore water. Enzyme activities are expressed as ratio between pDOC amended and unamended water. A ratio of 1: 1 means that activities were similar in the two treatments. * peptidase and glucosidase activities in the pDOC amended offshore experiment were not detectable.

treatment (Fig. 2A). In contrast, the two esterase activities (butyrate and oleate) in the coastal pDOC amendment were lower in the first week and at the same level in the second week compared with the unamended treatment. For the offshore pDOC treatment, all four enzyme activities gradually increased relative to the unamended treatment towards the end of the incubation (Fig. 2b). This pattern was most pronounced for glucosidase activities, reaching two orders of magnitude higher rates in the pDOC compared with the unamended treatment at day 15.

3.3. Changes in microbial community structure in response to pDOC

Bacterial communities at both sites were dominated by members of the bacterial phyla Pseudomonadota, Actinomycetota, and Bacteroidota that showed significantly lower relative abundances at the end of two treatments relative to their initial levels (Table 2). In the coastal water treatment, Verrucomicrobiota and Planctomycetota showed higher relative abundances in the pDOC treatment relative to the initial and the unamended water. The two latter phyla remained undetectable in the offshore experiment where members of the phyla Bacillota had higher relative abundances in the pDOC amendment compared with the initial and the unamended water.

3.4. Aggregation and sinking of marine plastic snow

Marine snow-type aggregates formed in roller tanks with both phytoplankton cultures (Fig. 3). *E. hux* aggregates were larger (0.45 ± 0.03 cm; $n = 4$) compared with those formed in the tank with *Isochrysis* sp. (0.16 ± 0.05 cm; $n = 5$) (Student's *t*-test, $p < 0.001$). *Isochrysis* sp. did not form visible aggregates with MPs, i.e., marine plastic snow. In contrast, *E. hux* and MPs formed marine plastic snow that had larger

Table 2
Top five abundant bacterial phyla in the experimental bottles with coastal and offshore water, containing natural levels of dissovlved organic carbon (DOC, unamended) and plastic-derived DOC (pDOC, amended). The last two columns represent the ratio for the increase or decrease of the phyla between the final (T_{end}) and initial time point ($T_{initial}$). Bolded numbers show statistically significant shift in relative abundance; a, b, c, d, e, g, h, i, j, k, n, o, p, q = $p < 0.001$; f, l, m = $p < 0.05$.

Sample	Phylum	Relative abundance (%)				
		$T_{initial}$	$T_{End\_unamended}$	$T_{End\_amended}$	$T_{End\_amended}$: $T_{initial}$	$T_{End\_unamended}$: $T_{initial}$
Coastal water	Pseudomonadota	**40**^{a}	71	**60**^{a}	1.5	1.8
	Actinomycetota	**24**^{b,c}	**2.6**^{b}	**1.7**^{c}	0.07	0.1
	Bacteroidota	**14**^{d,e}	**9.3**^{d}	**8**^{e}	0.6	0.7
	Planctomycetota	**1.5**^{f}	**0.4**^{f,g}	**8**^{g}	5.3	0.3
	Verrucomicrobiota	**1**^{h}	**0.5**^{i}	**13.8**^{h,i}	13.8	0.5
	Desulfobacterota	1	1.1	1.1	1.1	1.1
	Others	18.5	15.1	7.4	0.4	0.8
Offshore water	Pseudomonadota	**48.4**^{j}	**74.1**^{j,k}	**66.6**^{k}	1.4	1.5
	Actinomycetota	**15.4**^{l,m}	**6.4**^{l}	**2.3**^{m}	0.1	0.4
	Bacteroidota	**3.6**^{n,o}	**11**^{n}	**12**^{o}	3.3	3.1
	Bacillota	**6**^{p}	**1.7**^{p,q}	**9.7**^{q}	1.6	0.3
	Nitrospirota	1.4	0.4	1.9	1.4	0.3
	Others	25.2	6.4	7.5	0.3	0.3

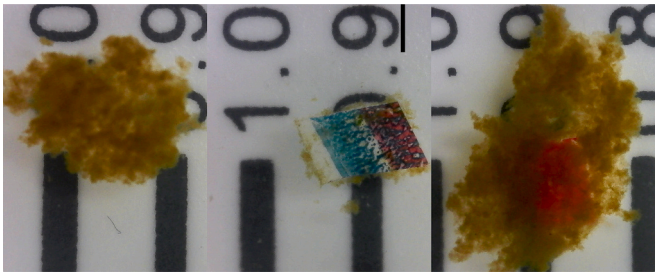

Fig. 3. Microscopic images of marine snow formed with *Emiliana huxleyi* (*E. hux*) (left); microplastic with *E. hux* cells (MP w/cells; middle) and *E. hux* marine snow with one piece of microplastic (marine plastic snow; right). The scale between the two black bars in each of the pictures is 1 mm.

average sizes (0.57 ± 0.04 cm; n = 4) compared with the *E. hux* marine snow (Student's t-test, $p < 0.01$). The fraction of MPs not associated with marine plastic snow had either visible biofilms (hereafter referred to as MPs w/cells; Fig. 3) or remained visually uncolonized (MPs w/o cells).

Average sinking velocities in the unstratified water column for the two types of marine snow ranged between 0.49 cm s^{-1} (*Isochrysis*) and 0.26 cm s^{-1} (*E. hux*) (Fig. 4a). Lower average sinking rates were found for marine plastic snow (0.22 cm s^{-1}), MPs w/cells (0.19 cm s^{-1}), and MPs w/o cells (0.11 cm s^{-1}).

Sinking velocities of marine snow and marine plastic snow in the density stratified sinking cylinder, calculated from the total transition time from the top to the bottom of the stratified water column, were reduced by the presence of the sharp density transition layer ($N = 2.1$ Hz) where all of the aggregates and MPS w/cells came to a stop (maximum residence time in the transition layer: 9 min). MPs w/o cells transitioned through the layer without stopping (visually discerned). Relative to the unstratified water column, sinking velocities in the stratified water column decreased by 73% for *E. hux* marine snow and marine plastic snow, 42% for MPs w/cells, 36% for MPs w/o cells, and 12% for *Isochrysis* marine snow (Fig. 4b).

4. Discussion

4.1. Microbial breakdown of pDOC

Our bioassays revealed site-specific differences in the drawdown of plastic-derived DOC (pDOC) with higher levels in the coastal compared with the offshore experiment. Romera-Castillo et al. (2018) reported a drawdown of 60% pDOC over 30 days in their seawater bottle experiments, and Zhu et al. (2020) found a range of 40% to 80% pDOC different types of plastics incubated in seawater over 92 days. The latter two studies were conducted under nutrient-replete conditions while our experiments were run without nutrient addition. In general, microbial degradation of pDOC is limited by the availability of N and P as plastic leachates have a high C and low N and P content. Offshore waters in the western Gulf of Maine in early fall when samples were collected, are generally low in N and P (Townsend et al., 2014), suggesting that microbial communities in our offshore experiment were nutrient limited, which could explain the lower extent in pDOC degradation relative to the coastal water experiment.

The weak growth response during pDOC drawdown in the first week of the incubations suggests that most of the C derived from plastic leachates was respired to CO_2 rather than incorporated into biomass. Rates and patterns of glucosidases and peptidases further indicate that a fraction of the acquired C from plastic leachates was repackaged and released as extracellular polymeric substances (EPS) enriched in carbohydrates and peptides. EPS are metabolic byproducts produced in response to a myriad of environmental conditions, including nutrient limitation and exposure to contaminants (Decho and Gutierrez, 2017). Production and release of EPS into the experimental water could also explain the presence of specific bacterial phyla such as Verrucomicrobiota and Planctomycetota that were enriched at the end of the coastal water pDOC treatment (Table 2). Members of these two phyla are known EPS degraders (Cardman et al., 2014; Martinez-Garcia et al., 2012; Sichert et al., 2020) and have been identified to colonize (Verrucomicrobiota; Marín et al., 2023) and degrade plastics in the ocean (Planctomycetota; Vaksmaa et al., 2022).

The presence of bacterial phyla involved with EPS degradation, together with the rates and patterns of EPS-hydrolyzing enzyme activities (glucosidases, peptidases), suggests that the addition of pDOC

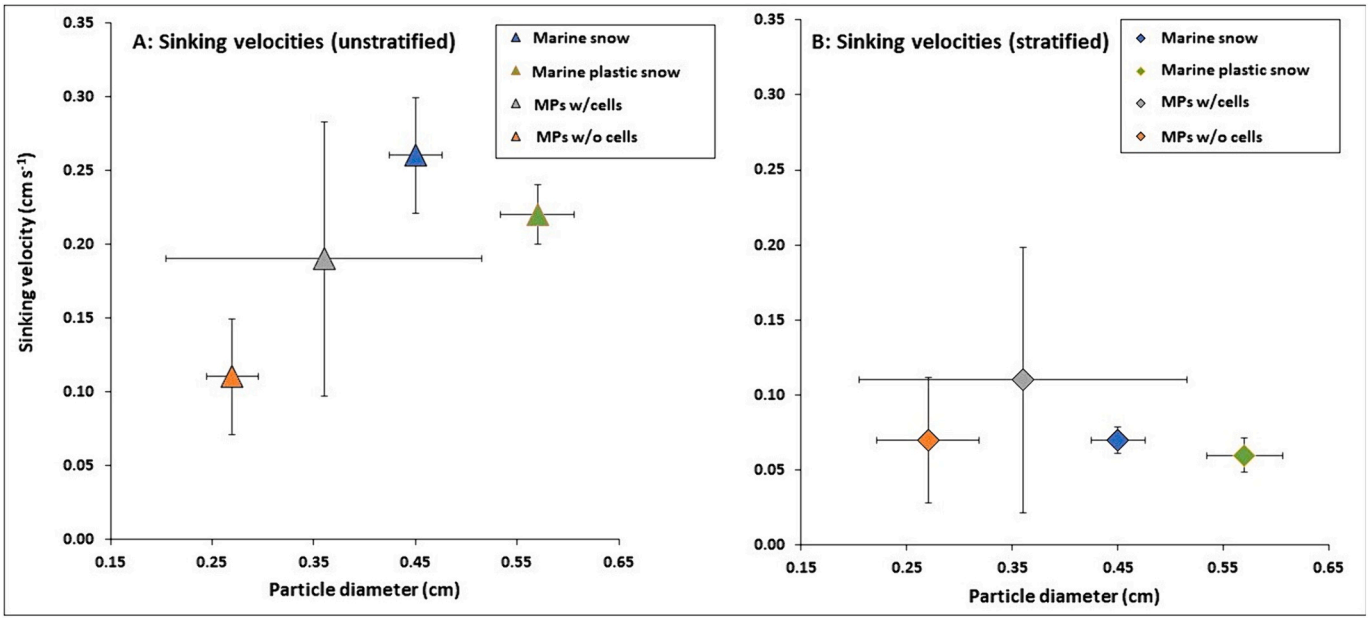

Fig. 4. Results from sinking velocities of the four types of particles ($n = 4$ for each particle type) in an unstratified (A) and density stratified water column (B). Note that results from *Isochrysis* aggregates are not included.

triggered a cascade of microbial responses (i.e., pDOC utilization followed by secondary consumers of metabolic byproducts – EPS) which has previously been described for oil-degrading microbial communities (Head et al., 2006) and documented in our earlier work on microbial degradation of oil-C in the Gulf of Mexico (Ziervogel et al., 2014; Ziervogel et al., 2012; Ziervogel and Arnosti, 2016). In the case of our offshore incubation, primary degradation of pDOC triggered substantial bacterial growth after a lag time of ~1 week, suggesting enhanced biomass production of secondary consumers fueled by EPS. Secondary consumers in the offshore experiment possibly included members of the phyla Bacillota that showed higher relative abundances in the amended relative to the unamended incubation (Table 2). Marine representatives of Bacillota have been shown to possess enzymatic capabilities to access and degrade carbohydrates and peptides (Bergauer et al., 2018).

Rates and patterns of the two esterases assayed here indicate that esterases were not involved with the utilization of pDOC and/or EPS, despite the fact that pDOC from polypropylene are primarily comprised of carboxylic acid-containing compounds (Stubbins et al., 2023), which are hydrolyzed by esterases. An alternative explanation for the disconnect between esterase activities and pDOC degradation is that esterase substrates within the pool of plastic leachates primarily consisted of low molecular weight compounds that did not require extracellular hydrolysis prior to uptake into the cell.

4.2. Formation and sinking of marine plastic snow

Phytoplankton interactions with MPs revealed species-specific differences in the formation of algal-MP aggregates (marine plastic snow). *Isochrysis* aggregates did not contain MPs, were smaller and appeared more fragile compared with *E. hux* aggregates that contained MPs, suggesting that the *E. hux* culture at the beginning of the roller tank incubations had a higher content of EPS compared with *Isochrysis*. The importance of EPS in the formation of marine plastic snow is supported by Galgani et al. (2022) who found a positive correlation between EPS and MPs in sediment traps containing marine plastic snow. EPS forms the underlying matrix for marine snow (Passow, 2002) and can occur as cell coatings or as discrete gel-like particles that increase particle 'stickiness' and thus particle coagulation efficiencies (Burd and Jackson, 2009). Moreover, EPS has been shown to exhibit nonpolar properties in the presence of hydrophobic compounds (Gutierrez et al., 2009) supporting the formation of biofilms onto MPs as observed here in the case of MPs w/cells (Fig. 3). The latter could have served as precursors for marine plastic snow in our roller tanks (Michels et al., 2018b).

Sinking velocities of marine plastic snow in the unstratified water column were almost double those of MPs, supporting the notion that vertically sinking marine plastic snow is an efficient transport vehicle for MPs (Galgani et al., 2022; Kvale et al., 2020; Long et al., 2015; Porter et al., 2018). The fact that marine plastic snow had a lower average sinking velocity compared with marine snow indicate that MPs potentially change the physical properties (e.g., density, drag) and export efficiencies of sinking C with consequences for the ocean C pump (Long et al., 2015; Porter et al., 2018).

In addition to their sinking velocities, the vertical distribution of aggregates in the water column is driven by the presence and strength of density gradients particularly in seasonally stratified, highly productive coastal waters and shelf seas (Alldredge et al., 2002; Möller et al., 2012; Prairie et al., 2017). In our study, stratification led to reduced average transit times from the surface to the denser bottom layer for all particle types tested here, as the sharp transition layer caused sinking particles to slow down or stop (Prairie et al., 2015). Accumulation of marine snow at density transition layers has been observed in the field and can result in particle thin layers that are hotspots for microbial degradation and zooplankton grazing (Alldredge et al., 2002; Möller et al., 2012; Prairie et al., 2017).

5. Conclusions

This study presents results from two separate laboratory experiments on two important pathways of plastic contaminants in the ocean: (i) photo-oxidation and the subsequent microbial utilization of dissolved plastic-derived compounds (pDOC), and (ii) sinking of marine plastic snow formed from MPs and phytoplankton cells. Our results suggest that the two pathways are linked through microbial EPS that are produced in response to pDOC utilization providing the 'glue' for marine plastic snow. The amount of EPS produced and thus their role in marine plastic snow formation, will ultimately depend on the levels of pDOC inputs. Direct measurements of the amount of pDOC (and EPS therefrom) relative to natural DOC have, to the best of our knowledge, not been made yet. Possible hotspots for inputs and microbial processing of pDOC are plastic-enriched surface waters such as subtropical gyres (Law, 2017). In these areas pDOC may yield significant amounts compared with natural DOC concentrations, particularly in the microlayer where less hydrophilic photoproducts such as carboxylic acids accumulate.

Understanding the effects of microbially mediated cycling of pDOC in plastic-rich surface waters may also be significant with respect to elemental stoichiometry and nutrient depletion. Assuming that all plastics floating at sea dissolved to DOC in a year (a vast overestimate of rates), this would yield a maximum input of 0.2 Pg-C (Stubbins et al., 2021), which is ~50 times less compared with DOC inputs from primary production (minimum estimate: ~12 Pg-C yr^{-1}; Dittmar and Stubbins, 2014). However, the addition of pDOC from photo-oxidized plastics would be a net input of DOC uncoupled from new production; its utilization and the subsequent microbial cascade of primary and secondary consumers as described here, would results in a net drawdown of nutrients. In the case of C limited systems, this nutrient drawdown from pDOC utilization would reduce resources for autotrophs limiting primary productivity (the 'more organic carbon gives less organic carbon' theory; Thingstad et al., 2008). A weakening of the efficiency of the biological C pump would potentially be amplified by marine plastic snow, reducing aggregate sinking rates and enhancing C attenuation, particularly in stratified waters as demonstrated here. Moreover, decreased aggregate transit times through stratified waters will increase the time for microbes and grazers to breakdown and ingest MPs, potentially leading to enhanced accumulation of marine plastic contaminants in higher trophic levels.

CRediT authorship contribution statement

Kai Ziervogel: Writing – review & editing, Writing – original draft, Project administration, Methodology, Investigation, Funding acquisition, Data curation, Conceptualization. **Sierra Kehoe:** Formal analysis. **Astrid Zapata De Jesus:** Formal analysis, Conceptualization. **Alireza Saidi-Mehrabad:** Writing – original draft, Formal analysis. **Miriam Robertson:** Formal analysis. **Ariana Patterson:** Formal analysis. **Aron Stubbins:** Writing – original draft, Methodology, Data curation, Conceptualization.

Data availability

Data will be made available on request.

Acknowledgments

We thank the captain of the RV Gulf Challenger and Shawn Shellito (UNH) for assistance with the sampling. We also thank Duane Moser (DRI) and Lixin Zhu (NU) for data discussions. Tracy Mandell (UNH) and Jobel Villafane (UH) helped with the sinking velocity measurements. Funding for this research came from UNH's Collaborative Research Excellence Initiative and the School of Marine Science and Ocean Engineering as well as NSF EPSCoR award# 1826734.

References

Alldredge, A.L., Silver, M.W., 1988. Characteristics, dynamics and significance of marine snow. Prog. Oceanogr. 20, 41–82.

Alldredge, A.L., Cowles, T.J., MacIntyre, S., Rines, J.E.B., Donaghay, P.L., Greenlaw, C.F., Holliday, D.V., Dekshenieks, M.M., Sullivan, J.M., Zaneveld, J.R.V., 2002. Occurrence and mechanisms of formation of a dramatic thin layer of marine snow in a shallow Pacific fjord. Mar. Ecol. Prog. Ser. 233, 1–12.

Andrady, A.L., 2011. Microplastics in the marine environment. Mar. Pollut. Bull. 62, 1596–1605. https://doi.org/10.1016/j.marpolbul.2011.05.030.

Andrady, A.L., Pegram, J.E., Searle, N.D., 1996. Wavelength sensitivity of enhanced photodegradable polyethylenes, ECO, and LDPE/MX. J. Appl. Polym. Sci. 62, 1457–1463.

Aoki, K., Furue, R., 2021. A model for the size distribution of marine microplastics: a statistical mechanics approach. PLoS One 16, e0259781. https://doi.org/10.1371/journal.pone.0259781.

Bergauer, K., Fernandez-Guerra, A., Garcia, J.A.L., Sprenger, R.R., Stepanauskas, R., Pachiadaki, M.G., Jensen, O.N., Herndl, G.J., 2018. Organic matter processing by microbial communities throughout the Atlantic water column as revealed by metaproteomics. Proceed. National Acad. Sci. 115, E400. https://doi.org/10.1073/pnas.1708779115.

Burd, A.B., Jackson, G.A., 2009. Particle Aggregation. Annu. Rev. Mar. Sci. 1, 65–90 doi: 10.1146/annurev.marine.010908.163904.

Callahan, B.J., McMurdie, P.J., Rosen, M.J., Han, A.W., Johnson, A.J.A., Holmes, S.P., 2016. DADA2: high-resolution sample inference from Illumina amplicon data. Nat. Methods 13, 581–583. https://doi.org/10.1038/nmeth.3869.

Caporaso, J.G., Lauber, C.L., Walters, W.A., Berg-Lyons, D., Huntley, J., Fierer, N., Owens, S.M., Betley, J., Fraser, L., Bauer, M., Gormley, N., Gilbert, J.A., Smith, G., Knight, R., 2012. Ultra-high-throughput microbial community analysis on the Illumina HiSeq and MiSeq platforms. ISME J. 6, 1621–1624. https://doi.org/10.1038/ismej.2012.8.

Cardman, Z., Arnosti, C., Durbin, A., Ziervogel, K., Cox, C., Steen, A.D., Teske, A., 2014. Verrucomicrobia are candidates for polysaccharide-degrading bacterioplankton in an Arctic Fjord of Svalbard. Appl. Environ. Microbiol. 80, 3749. https://doi.org/10.1128/AEM.00899-14.

Chrost, R.J. (Ed.), 1991. Microbial Enzymes in Aquatic Environments. Springer Verlag, New York.

Cózar, A., Echevarría, F., González-Gordillo, J.I., Irigoien, X., Úbeda, B., Hernández-León, S., Palma, Á.T., Navarro, S., García-de-Lomas, J., Ruiz, A., Fernández-de-Puelles, M.L., Duarte, C.M., 2014. Plastic debris in the open ocean. Proceed. National Acad. Sci. 201314705 https://doi.org/10.1073/pnas.1314705111.

Decho, A.W., Gutierrez, T., 2017. Microbial extracellular polymeric substances (EPSs) in ocean systems. Front. Microbiol. 8, 922. https://doi.org/10.3389/fmicb.2017.00922.

Dittmar, T., Stubbins, A., 2014. 12.6 - dissolved organic matter in aquatic systems. In: Holland, H.D., Turekian, K.K. (Eds.), Treatise on Geochemistry, Second edition. Elsevier, pp. 125–156.

Galgani, L., Goßmann, I., Scholz-Böttcher, B., Jiang, X., Liu, Z., Scheidemann, L., Schlundt, C., Engel, A., 2022. Hitchhiking into the deep: How microplastic particles are exported through the biological carbon pump in the North Atlantic Ocean. Environ. Sci. Technol. 56, 15638–15649. https://doi.org/10.1021/acs.est.2c04712.

Gasol, J.M., Del Giorgio, P.A., 2000. Using flow cytometry for counting natural planktonic bacteria and understanding the structure of planktonic bacterial communities. Sci. Mar. 64, 197–224. https://doi.org/10.3989/scimar.2000.64n2197.

Gewert, B., Plassmann, M.M., MacLeod, M., 2015. Pathways for degradation of plastic polymers floating in the marine environment. Environ Sci Process Impacts 17, 1513–1521. https://doi.org/10.1039/C5EM00207A.

Gewert, B., Plassmann, M., Sandblom, O., MacLeod, M., 2018. Identification of chain scission products released to water by plastic exposed to ultraviolet light. Environ. Sci. Technol. Lett. 5, 272–276. https://doi.org/10.1021/acs.estlett.8b00119.

Gutierrez, T., Morris, G., Green, D.H., 2009. Yield and physicochemical properties of EPS from *Halomonas* sp. strain TG39 identifies a role for protein and anionic residues (sulfate and phosphate) in emulsification of n-hexadecane. Biotechnol. Bioeng. 103, 207–216. https://doi.org/10.1002/bit.22218.

Head, I.M., Jones, D.M., Röling, W.F.M., 2006. Marine microorganisms make a meal of oil. Nat. Rev. Microbiol. 4, 173–182.

Hermabessiere, L., Dehaut, A., Paul-Pont, I., Lacroix, C., Jezequel, R., Soudant, P., Duflos, G., 2017. Occurrence and effects of plastic additives on marine environments and organisms: a review. Chemosphere 182, 781–793. https://doi.org/10.1016/j.chemosphere.2017.05.096.

Hoppe, H.-G., 1983. Significance of exoenzymatic activities in the ecology of brackish water: measurements by means of methylumbelliferyl-substrates. Mar. Ecol. Prog. Ser. 11, 299–308. https://doi.org/10.3354/meps011299.

Kvale, K., Prowe, A.E.F., Chien, C.-T., Landolfi, A., Oschlies, A., 2020. The global biological microplastic particle sink. Sci. Rep. 10, 16670. https://doi.org/10.1038/s41598-020-72898-4.

Laurenceau-Cornec, E.C., Trull, T.W., Davies, D.M., De La Rocha, C.L., Blain, S., 2015. Phytoplankton morphology controls on marine snow sinking velocity. Mar. Ecol. Prog. Ser. 520, 35–56.

Law, K.L., 2017. Plastics in the marine environment. Annu. Rev. Mar. Sci. 9, 205–229. https://doi.org/10.1146/annurev-marine-010816-060409.

Long, M., Moriceau, B., Gallinari, M., Lambert, C., Huvet, A., Raffray, J., Soudant, P., 2015. Interactions between microplastics and phytoplankton aggregates: impact on their respective fates. Mar. Chem. 175, 39–46. https://doi.org/10.1016/j.marchem.2015.04.003.

Mandel, T.L., Zhou, D.Z., Waldrop, L., Theillard, M., Kleckner, D., Khatri, S., 2020. Retention of rising droplets in density stratification. Phys. Rev. Fluids 5, 124803.

Marín, A., Feijoo, P., de Llanos, R., Carbonetto, B., González-Torres, P., Tena-Medialdea, J., García-March, J.R., Gámez-Pérez, J., Cabedo, L., 2023. Microbiological characterization of the biofilms colonizing bioplastics in natural marine conditions: a comparison between PHBV and PLA. Microorganisms 11. https://doi.org/10.3390/microorganisms11061461.

Martinez-Garcia, M., Brazel, D.M., Swan, B.K., Arnosti, C., Chain, P.S.G., Reitenga, K.G., Xie, G., Poulton, N.J., Gomez, M.L., Masland, D.E.D., Thompson, B., Bellows, W.K., Ziervogel, K., Lo, C.-C., Ahmed, S., Gleasner, C.D., Detter, C.J., Stepanauskas, R., 2012. Capturing single cell genomes of active polysaccharide degraders: an unexpected contribution of Verrucomicrobia. PLoS One 7, e35314. https://doi.org/10.1371/journal.pone.0035314.

Michels, J., Stippkugel, A., Lenz, M., Wirtz, K., Engel, A., 2018a. Rapid aggregation of biofilm-covered microplastics with marine biogenic particles. Proc. R. Soc. B Biol. Sci. 285 https://doi.org/10.1098/rspb.2018.1203, 20181203.

Michels, J., Stippkugel, A., Lenz, M., Wirtz, K., Engel, A., 2018b. Rapid aggregation of biofilm-covered microplastics with marine biogenic particles. Proc. R. Soc. B Biol. Sci. 285 https://doi.org/10.1098/rspb.2018.1203, 20181203.

Möller, K.O., St John, M., Temming, A., Floeter, J., Sell, A.F., Herrmann, J.P., Möllmann, C., 2012. Marine snow, zooplankton and thin layers: indications of a trophic link from small-scale sampling with the video plankton recorder. Mar. Ecol. Prog. Ser. 468, 57–69.

Passow, U., 2002. Transparent exopolymer particles (TEP) in aquatic environments. Prog. Oceanogr. 55, 287–333. https://doi.org/10.1016/S0079-6611(02)00138-6.

Porter, A., Lyons, B.P., Galloway, T.S., Lewis, C., 2018. Role of marine snows in microplastic fate and bioavailability. Environ. Sci. Technol. 52, 7111–7119. https://doi.org/10.1021/acs.est.8b01000.

Prairie, J.C., Ziervogel, K., Camassa, R., McLaughlin, R.M., White, B.L., Dewald, C., Arnosti, C., 2015. Delayed settling of marine snow: effects of density gradient and particle properties and implications for carbon cycling. Mar. Chem. 175, 28–38. https://doi.org/10.1016/j.marchem.2015.04.006.

Prairie, J.C., Ziervogel, K., Camassa, R., McLaughlin, R.M., White, B.L., Johnson, Z.I., Arnosti, C., 2017. Ephemeral aggregate layers in the water column leave lasting footprints in the carbon cycle. Limnol. and Oceanogra. Lett. 2, 202–209. https://doi.org/10.1002/lol2.10053.

Pruesse, E., Quast, C., Knittel, K., Fuchs, B.M., Ludwig, W., Peplies, J., Glöckner, F.O., 2007. SILVA: a comprehensive online resource for quality checked and aligned ribosomal RNA sequence data compatible with ARB. Nucleic Acids Res. 35, 7188–7196. https://doi.org/10.1093/nar/gkm864.

Repeta, D.J., 2015. Chapter 2 - chemical characterization and cycling of dissolved organic matter. In: Hansell, D.A., Carlson, C.A. (Eds.), Biogeochemistry of Marine Dissolved Organic Matter, Second edition. Academic Press, Boston, pp. 21–63. https://doi.org/10.1016/B978-0-12-405940-5.00002-9.

Romera-Castillo, C., Pinto, M., Langer, T.M., Álvarez-Salgado, X.A., Herndl, G.J., 2018. Dissolved organic carbon leaching from plastics stimulates microbial activity in the ocean. Nat. Commun. 9, 1430. https://doi.org/10.1038/s41467-018-03798-5.

Saidi-Mehrabad, A., Neuberger, P., Cavaco, M., Froese, D., Lanoil, B., 2020. Optimization of subsampling, decontamination, and DNA extraction of difficult peat and silt permafrost samples. Sci. Rep. 10, 14295. https://doi.org/10.1038/s41598-020-71234-0.

Schloss, P.D., Westcott, S.L., Ryabin, T., Hall, J.R., Hartmann, M., Hollister, E.B., Lesniewski, R.A., Oakley, B.B., Parks, D.H., Robinson, C.J., Sahl, J.W., Stres, B., Thallinger, G.G., Van Horn, D.J., Weber, C.F., 2009. Introducing mothur: open-source, platform-independent, community-supported software for describing and comparing microbial communities. Appl. Environ. Microbiol. 75, 7537–7541. https://doi.org/10.1128/AEM.01541-09.

Shanks, A.L., Edmondson, E.W., 1989. Laboratory-made artificial marine snow: a biological model of the real thing. Mar. Biol. 101, 463–470.

Sheridan, E.A., Fonvielle, J.A., Cottingham, S., Zhang, Y., Dittmar, T., Aldridge, D.C., Tanentzap, A.J., 2022. Plastic pollution fosters more microbial growth in lakes than natural organic matter. Nat. Commun. 13, 4175. https://doi.org/10.1038/s41467-022-31691-9.

Sichert, A., Corzett, C., Schechter, M., Unfried, F., Markert, S., Becher, D., Fernandez-Guerra, A., Liebeke, M., Schweder, T., Polz, M., Hehemann, J.-H., 2020. Verrucomicrobia use hundreds of enzymes to digest the algal polysaccharide fucoidan. Nat. Microbiol. 5, 1–14. https://doi.org/10.1038/s41564-020-0720-2.

Simon, M., Grossart, H.P., Schweitzer, B., Ploug, H., 2002. Microbial ecology of organic aggregates in aquatic ecosystems. Aquat. Microb. Ecol. 28, 175–211.

Stubbins, A., Dittmar, T., 2012. Low volume quantification of dissolved organic carbon and dissolved nitrogen. Limnol. Oceanogr. Methods 10, 347–352. https://doi.org/10.4319/lom.2012.10.347.

Stubbins, A., Law, K.L., Muñoz, S.E., Bianchi, T.S., Zhu, L., 2021. Plastics in the earth system. Science 373, 51–55. https://doi.org/10.1126/science.abb0354.

Stubbins, A., Zhu, L., Zhao, S., Spencer, R.G.M., Podgorski, D.C., 2023. Molecular signatures of dissolved organic matter generated from the Photodissolution of microplastics in sunlit seawater. Environ. Sci. Technol. 57, 20097–20106. https://doi.org/10.1021/acs.est.1c03592.

Thingstad, T.F., Bellerby, R.G.J., Bratbak, G., Børsheim, K.Y., Egge, J.K., Heldal, M., Larsen, A., Neill, C., Nejstgaard, J., Norland, S., Sandaa, R.-A., Skjoldal, E.F., Tanaka, T., Thyrhaug, R., Töpper, B., 2008. Counterintuitive carbon-to-nutrient coupling in an Arctic pelagic ecosystem. Nature 455, 387–390. https://doi.org/10.1038/nature07235.

Townsend, D.W., McGillicuddy, D.J., Thomas, M.A., Rebuck, N.D., 2014. Nutrients and water masses in the Gulf of Maine–Georges Bank region: Variability and importance

to blooms of the toxic dinoflagellate *Alexandrium fundyense*. Deep-Sea Res. II Top. Stud. Oceanogr. 103, 238–263. https://doi.org/10.1016/j.dsr2.2013.08.003.

Vaksmaa, A., Egger, M., Lüke, C., Martins, P.D., Rosselli, R., Asbun, A.A., Niemann, H., 2022. Microbial communities on plastic particles in surface waters differ from subsurface waters of the North Pacific subtropical gyre. Mar. Pollut. Bull. 182, 113949 https://doi.org/10.1016/j.marpolbul.2022.113949.

Wang, Q., Garrity, G.M., Tiedje, J.M., Cole, J.R., 2007. Naïve Bayesian classifier for rapid assignment of rRNA sequences into the new bacterial taxonomy. Appl. Environ. Microbiol. 73, 5261–5267. https://doi.org/10.1128/AEM.00062-07.

Zhang, H., Perez-Garcia, P., Dierkes, R.F., Applegate, V., Schumacher, J., Chibani, C.M., Sternagel, S., Preuss, L., Weigert, S., Schmeisser, C., Danso, D., Pleiss, J., Almeida, A., Höcker, B., Hallam, S.J., Schmitz, R.A., Smits, S.H.J., Chow, J., Streit, W.R., 2022. The Bacteroidetes *Aequorivita* sp. and *Kaistella jeonii* produce promiscuous esterases with PET-hydrolyzing activity. Front. Microbiol. 12 https://doi.org/10.3389/fmicb.2021.803896.

Zhenfeng, Z., Xingzhou, H., Zubo, L., 1996. Wavelength sensitivity of photooxidation of polypropylene. Polym. Degrad. Stab. 51, 93–97. https://doi.org/10.1016/0141-3910(95)00210-3.

Zhu, L., Zhao, S., Bittar, T.B., Stubbins, A., Li, D., 2020. Photochemical dissolution of buoyant microplastics to dissolved organic carbon: rates and microbial impacts. J. Hazard. Mater. 383, 121065 https://doi.org/10.1016/j.jhazmat.2019.121065.

Ziervogel, K., Arnosti, C., 2016. Enhanced protein and carbohydrate hydrolysis in plume-associated deep waters initially sampled during the early stages of the Deepwater horizon oil spill. Deep-Sea Res. II Top. Stud. Oceanogr. https://doi.org/10.1016/j.dsr2.2013.09.003.

Ziervogel, K., McKay, L., Rhodes, B., Osburn, C.L., Dickson-Brown, J., Arnosti, C., Teske, A., 2012. Microbial activities and dissolved organic matter dynamics in oil-contaminated surface seawater from the Deepwater horizon oil spill site. PLoS One 7, e34816. https://doi.org/10.1371/journal.pone.0034816.

Ziervogel, K., D'souza, N., Sweet, J., Yan, B., Passow, U., 2014. Natural oil slicks fuel surface water microbial activities in the northern Gulf of Mexico. Front. Microbiol. 5 https://doi.org/10.3389/fmicb.2014.00188.